Article

Evaluating the Curtailment Risk of Non-Firm Utility-Scale Solar Photovoltaic Plants under a Novel Last-In First-Out Principle of Access Interconnection Agreement

Kwami Senam A. Sedzro *, Kelsey Horowitz, Akshay K. Jain, Fei Ding, Bryan Palmintier and Barry Mather

National Renewable Energy Laboratory, Golden, CO 80401, USA; khorowitz@nrel.gov or
kelsey.a.w.horowitz@gmail.com (K.H.); akjain@vt.edu (A.K.J.); Fei.Ding@nrel.gov (F.D.);
Bryan.Palmintier@nrel.gov (B.P.); Barry.Mather@nrel.gov (B.M.)
* Correspondence: ksedzro@ieee.org

Abstract: AbstractsWith the increasing share of distributed energy resources on the electric grid, utility companies are facing significant decisions about infrastructure upgrades. An alternative to extensive and capital-intensive upgrades is to offer non-firm interconnection opportunities to distributed generators, via a coordinated operation of utility scale resources. This paper introduces a novel flexible interconnection option based on the last-in, first-out principles of access aimed at minimizing the unnecessary non-firm generation energy curtailment by balancing access rights and contribution to thermal overloads. Although we focus on solar photovoltaic (PV) plants in this work, the introduced flexible interconnection option applies to any distributed generation technology. The curtailment risk of individual non-firm PV units is evaluated across a range of PV penetration levels in a yearlong quasi-static time-series simulation on a real-world feeder. The results show the importance of the size of the curtailment zone in the curtailment risk distribution among flexible generation units as well as that of the "access right" defined by the order in which PV units connect to the grid. Case study results reveal that, with a proper selection of curtailment radius, utilities can reduce the total curtailment of flexible PV resources by up to more than 45%. Findings show that non-firm PV generators can effectively avoid all thermal limit-related upgrade costs.

Keywords: renewable integration; distributed PV integration; active network management; PV interconnection agreement

1. Introduction

Electric power distribution systems are traditionally designed and planned to move energy from the distribution substation to end users. In this design, all the energy needs from consumers are centrally supplied. With the increased interest in distributed energy resources (DERs), distribution system operators (DSOs) are receiving increasing numbers of customer generation applications. These customers, commonly referred to as prosumers, own generation assets on their premises. Often, these assets are solar photovoltaic (PV) plants as a result of their modularity, decreasing solar panel prices, and state incentives. The size of such installations varies as a function of customer type (residential, commercial, or industrial), socioeconomic standing, etc. For a DSO or utility company, the challenge is to evaluate the potential impacts each customer-owned generation asset might have on the safe and reliable operation of the distribution system, which was originally conceived assuming one-way power flow. That is the aim of the interconnection studies DSOs perform as part of the interconnection application review process. Two main interconnection categories have been implemented to date: firm interconnection and flexible interconnection.

Firm interconnection is the most common and most widely adopted option worldwide. In this category, applications are reviewed considering all potential technical challenges. Applicants that pass the tests are given unrestricted access to the network within the limits

of the regulation that governs such interconnections. Interconnection applications that fail one or more screening tests are rejected or recommended mitigation strategies that would alleviate the violations suspected. Network constraint mitigation strategies can be costly and can make the project economically nonviable [1]. If the applicant is willing and able to pay for the needed upgrade, the application will be given due attention and the upgrades implemented before interconnection; otherwise, the application is denied, or the project is cancelled. Connected firm generators are not subject to curtailment signals from the DSO.

To relieve the burden of high connection costs on energy project developers and optimize the use of existing network infrastructure, flexible interconnection options have recently emerged and have been more frequently implemented in Europe via so-called active network management platforms [2]. Flexible interconnection options offer an applicant the opportunity to avoid upgrades by accepting that its system's real power output might be subject to curtailment as necessary to avoid system violations. These options generally include DER management systems, in which optimal active and reactive power set points are determined through online system operational optimization; and principles of access (PoA), in which the real power output of interconnected variable resources is curtailed as needed according to market- or nonmarket-based approaches. A market-based approach suggests the creation of a curtailment market where flexible generators bid for curtailment and get compensated according to the established market rules [3]. This approach is impractical in the short term at the distribution level because it requires a formal distribution power market arrangement. Nonmarket approaches include [4]:

- *Last-in, first-out (LiFo)*: the last non-firm generator to connect is the first to be curtailed in case a network constraint is violated, and the first to connect is the last to be curtailed if the violation persists.
- *Pro rata*: the required curtailment volume is equally distributed among all non-firm generators.
- *Shedding rota*: curtails non-firm generators in a predefined rotational order updated on a regular basis (e.g., every day).
- *Technical best*: curtailment is assigned to non-firm generators based on their contribution to the network constraint violation.
- *Greatest carbon benefit*: curtailment is assigned to non-firm generators based on their carbon emission levels with the objective to minimize overall carbon emission.
- *Most convenient*: generators are curtailed based on the DSO's preference, i.e., which could be because of convenience and effectiveness.
- *Generator size*: the first generator to be curtailed is the one with the highest output that is contributing to the violation.

These options have been explored in the United Kingdom. In the United States, the City of New York is currently piloting the flexible interconnect capacity solution with two *DER* projects: one 2 MW PV plant and one 450 kW farm waste digestor [5]. A detailed survey of different arrangements and associated issues is presented in [4,6,7]. Additionally, based on the U.K. experience, the *LiFo*, pro rata, or a combination of both methods, with generators placed in tranches with different levels of maximum curtailment according to when they interconnected have previously, been the most acceptable options. *LiFo* has been the most prevailing form in distribution networks in the United Kingdom [8,9], even though it might not always be the most economically efficient option [10]. In fact, *LiFo* presents many drawbacks. UK Power Networks, a distribution system operator, investigated alternative arrangements in the Flexible Plug and Play project. The study concluded that despite the simplicity of the *LiFo* arrangement, pro rata curtailment would be more attractive for subsequent non-firm renewable generators [4]. One drawback of *LiFo* is that it does not account for generator location when defining curtailment priorities, as highlighted in [11]. This leads to systematically high curtailment risk for later connected non-firm generators, even if they are not contributing to a given grid constraint. Potential solutions to this issue include the use of power flow sensitivity factors, as proposed in [12]. Although combining this approach with *LiFo* would yield a better performance than the

current *LiFo* approach, it would be more computationally expensive and might become infeasible for implementation in large distribution systems. In addition, the most attractive feature of the *LiFo*, which is simplicity, might be lost. To be "fairer" in the *LiFo* curtailment allocation, this paper introduces a novel electric distance-based, last-in, first-out (*ed-LiFo*) *PoA*. In this approach, curtailment signals, instead of being solely based on the rank of access to the distribution network, consider the proximity of candidate generators to the location of the thermal overloads as a proxy for their contribution level to the network constraints. The aim of this work, beyond the innovative *ed-LiFo* option, is to assess the curtailment risk of non-firm, large-scale PV plants. In addition to thermal violations, voltage issues can arise with distributed resource integration [13]. These might not always be resolved using the *LiFo* curtailment scheme. Therefore, in this paper, we use an advanced inverter with autonomous Volt-VAR settings to control the voltage at PV nodes.

In summary, the contribution of this paper is twofold:

- First, we introduce a novel flexible interconnection scheme based on the *LiFo* framework with the objective to minimize unnecessary curtailment of non-firm generation resources while considering the access rights of individual flexible generation units.
- Second, we evaluate the curtailment risk distribution among flexible units at different PV penetration levels in an annual quasi-static time-series (*QSTS*) distribution system simulation framework.

The remainder of this paper is organized as follows. Section 2 presents the methodology of the proposed non-firm interconnection scheme. Section 3 describes the distribution test system and the test setups considered in our case study. Section 4 analyses the observations from the case study results, and discusses the insights derived. Section 5 concludes the paper.

2. Methodology

The proposed flexible interconnection option, *ed-LiFo*, refers to a non-firm PV connection scheme that schedules PV real power curtailment according to the non-firm generators' network access order (as in the traditional *LiFo*) while considering their proximity to the thermal violation observed. Section 2.1 presents the concept of electrical distance considered in this paper.

2.1. Electrical Distance

Klein and Randić introduced the concept of resistance distance, generally referred to as electrical distance [14]. Considering a connected graph, G, defined by a set of vertices, V, and a set of edges, the authors placed a unit resistance on each edge (i, j). The resistance distance between two vertices is the effective resistance (or Thevenin resistance) obtained using the standard series and parallel equivalents reduction techniques. For the sake of quantifying the proximity of two nodes, we consider the distribution network as a conductance (inverse of the resistance) weighted graph G. The adjacency matrix A of G, assuming n vertices, has the form given in (1), where g_{ij} is the conductance that connects vertices i and j. g_{ij} is nonzero only if the edge i–j exists.

$$A = \begin{bmatrix} 0 & \cdots & g_{1n} \\ \vdots & \ddots & \vdots \\ g_{n1} & \cdots & 0 \end{bmatrix} \tag{1}$$

As shown in (1), A is a square matrix with diagonal filled with zeros.

We define a diagonal matrix called "degree" matrix D, which features the strength of ties of a node i in G. The degree of node i is the sum of the conductance elements that connect i to other nodes, with elements D_{ii} given by (2):

$$D_{ii} = \sum_{j \in V, \, j \neq i} g_{ij} \tag{2}$$

The Laplacian matrix derived from this representation is shown in (3) and is the conductance matrix, or the "real part" of the classic admittance matrix in electric circuit theory, as given in (4):

$$L = D - A \tag{3}$$

$$L_{ik} = \begin{cases} \sum_{j \in V} g_{ij}, & if \quad i = k \\ -g_{ik}, & if \ i \neq k \end{cases} \tag{4}$$

The electrical distance matrix E is defined by (5):

$$E_{ik} = L_{ii}^\dagger + L_{kk}^\dagger - L_{ik}^\dagger - L_{ki}^\dagger \tag{5}$$

where E_{ij} is the resistance distance between nodes i and j; $L^\dagger$ is the pseudo- or group inverse of the Laplacian matrix L. As the Laplacian matrix (conductance matrix, in our case) is real-symmetric, the existence of its pseudo-inverse is guaranteed [15–17]. The relationship between L and $L^\dagger$ is defined by the properties shown in (6) [18]:

$$\begin{aligned} LL^\dagger L &= L \\ L^\dagger LL^\dagger &= L^\dagger \\ LL^\dagger &= L^\dagger L \end{aligned} \tag{6}$$

2.2. ed-LiFo PoA

The aim of the proposed *ed-LiFo* is to reduce unnecessary curtailments, i.e., the curtailment of generators that do not contribute to the thermal constraints experienced. In fact, with the traditional *LiFo* scheme, early connected non-firm generators, even if sited in constrained network areas, would be exposed to relatively less curtailment risk, whereas the later connected non-firm generators located in less restricted areas are exposed to increased curtailment risk. The proposed *ed-LiFo* is based on active curtailment zone formation. A violation zone is dynamically identified as the union of a set of nodes within a given radius of all nodes directly connected to an overloaded line within the distribution system. Figure 1 is an illustration of a violation zone formation—physical distances are used in this illustration for easy visual representation.
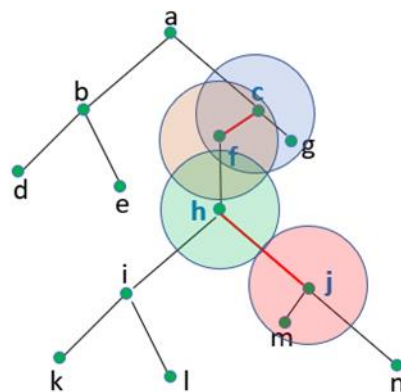

Figure 1. Violation zone formation.

In this illustration, lines (c, f) and (h, j) experience thermal violation. Hence, the set of nodes that are directly connected to any thermal violation is $DCN = \{c, f, h, j\}$. With a preset curtailment zone radius, ρ, individual violation areas represented by ρ-radius discs centered in each directly connected node are determined. Any non-firm generator located at a node that falls on a disc is a candidate for curtailment. The set of nodes CCN at which non-firm generators are subject to curtailment is given by (7):

$$(z \in CCN) \Longleftrightarrow (E_{zt} \leq \rho), \exists t \in DCN, \forall z \in V \tag{7}$$

In Figure 1, the set of curtailment candidate nodes is $CCN = \{c, f, g, h, j, m\}$. The set of PV units, candidate to curtailment in their *LiFo* order, is given by (8):

$$CCPV = LiFo(\{PV_i, \forall \ PV_i \ located \ at \ any \ bus \ in \ CCN\}) \tag{8}$$

Consequently, any non-firm generator located at any *CCN* node might receive a curtailment signal from the distribution system operator. This assumes that this feeder hosts a set four non-firm PV units $\{PV_d, PV_f, PV_h, PV_k, PV_m, PV_n\}$ located, respectively, at d, f, h, k, m, and n, in order of connection, with PV_d the first and PV_n the last. As d, k, and n are not in *CCN*, even though PV_n is the last to connect to the feeder, it will not be curtailed unless all curtailment PV candidates have been curtailed and the thermal overloads still exist. In fact, in practice, all non-firm generators that are not curtailment candidates are appended to *CCPV* in their *LiFo* order. This way, in case the candidate list is exhausted before overload is relieved, non-curtailment candidates might receive curtailment signals.

The curtailment order will be given by the set of curtailment candidate PV systems *CCPV* as follows $\{PV_m, PV_h, PV_f\}$. The augmented *CCPV* would include PV_n, PV_k, and PV_d at the end according to their *LiFo* order. Thus, if none of the candidates can suppress the thermal violation, PV_n, PV_k, and PV_d will receive curtailment signals in this order. The set of curtailment candidates, *CCPV*, will then be $\{PV_m, PV_h, PV_f, PV_n, PV_k, PV_d\}$.

To select the curtailment zone radius ρ discussed in (7), we introduce (9):

$$\rho = \mu + r\sigma \tag{9}$$

where μ and σ are, respectively, the average and standard deviation of the set of electrical distance values between any two buses in the feeder, and r is a railing factor. To ensure a feasible choice of curtailment zone radius, r must satisfy constraint (10):

$$-\frac{\mu}{\sigma} \leq r \leq \frac{E_{max} - \mu}{\sigma} \tag{10}$$

where E_{max} is the electrical diameter of the feeder, i.e., the maximum electrical distance between any two buses of the feeder.

Figure 2 describes the *ed-LiFo PoA* framework and its implementation in a *QSTS* simulation. The shaded boxes identify *ed-LiFo* processes.

When the system approaches a preset thermal limit, either on lines or transformers, the *ed-LiFo PoA* control is activated. Curtailment decisions are made and executed until thermal violations are suppressed. This concept is tested in Section 3.
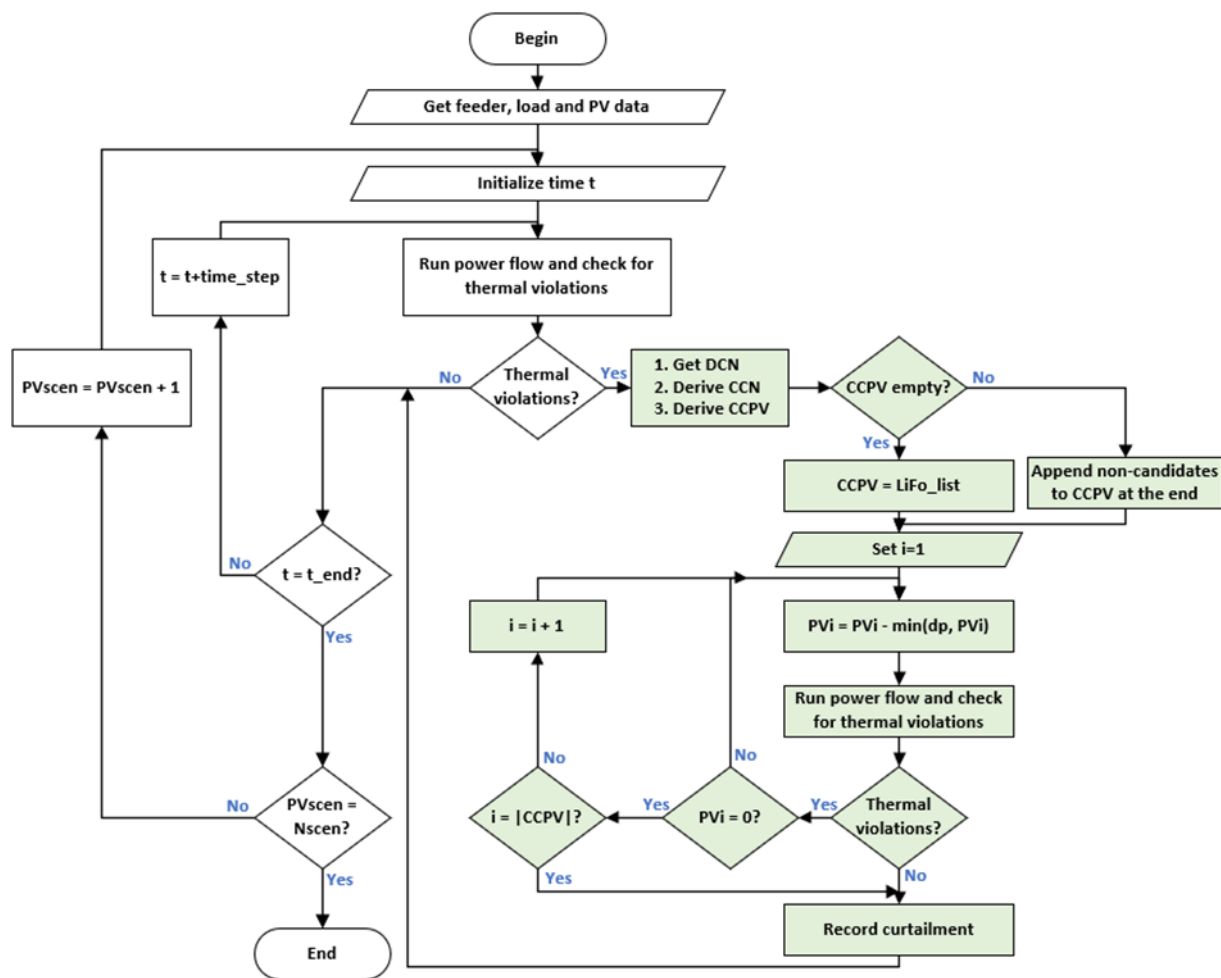
Figure 2. Electric distance-based, last-in, first-out (*ed-LiFo*) flowchart in a quasi-static time-series (*QSTS*) simulation for photovoltaic (PV) curtailment risk assessment.

3. Case Study

To evaluate the proposed flexible interconnection option and determine the curtailment risk incurred by non-firm generators, we consider an example on a real-word test feeder, a PV scenario as well as the *ed-LiFo* design described in Sections 3.1–3.3.

3.1. Distribution Feeder

The study presented in this paper applies to the utility distribution feeder shown in Figure 3, the same as Feeder A studied in [19]. It is a 12.47 kV distribution system feeding 291 residential customers and 334 commercial customers, for a total load of 7.65 megawatts. The farthest customer is at 9.7 km from the substation. The primary bus X/R ratio ranges from 0.669 to 5.71 with an average of 2.206. In this test feeder, voltage support is provided by 6 capacitor units totaling 4800 kVAR in capacity. It should be noted that no line regulator nor load tap changer is present. The electrical connectivity within the studied feeder is presented in Figure 4, by means of the cumulative density function of the electrical distance given in Equation (5) and features the electrical distance between any two buses. The normalized load profile used in this case study is obtained from supervisory control and data acquisition system measurements. We use a single PV profile based on measured irradiation data at a station near the test feeder. We assume that the topology of the feeder does not change throughout the year.
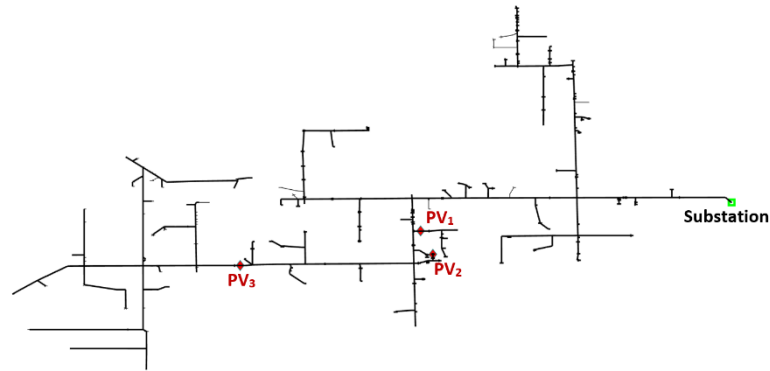
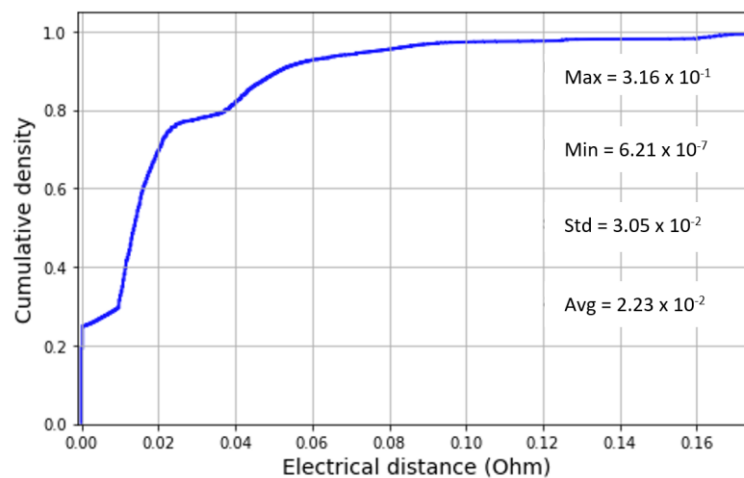**Figure 3.** Topology of the test feeder and location of utility scale PV units.

Figure 4. Cumulative distribution function of electrical distances within the test feeder.

3.2. PV Scenarios

We consider a set of three identical large-scale PV units with size starting at 500 kW. The location of the PV systems is randomly chosen and fixed, as shown in Figure 3, across all penetration levels. Higher PV penetration levels (percentage PV to peak load ratio) are obtained by increasing the size of each PV unit by 50 kW at a time. We use real-world load and solar irradiation profiles to conduct a yearlong simulation at a 1-min time resolution. Each PV unit is a three-phase system equipped with a Volt-VAR controlled inverter. The Volt-VAR control satisfies the standard for interconnection and interoperability of distributed energy resources published by the Institute Electrical and Electronics Engineers (IEEE). We use the default IEEE 1547–2018 Category A Volt-VAR curve shown in Figure 5.

In the *ed-LiFo* study case, where the active power output of a PV unit can be completely curtailed at times, the maximum reactive power available is limited to 25% of the inverter apparent power rating according to the IEEE 1547–2018 standard (Table 8, p. 39). This ensures a category A Volt-VAR local voltage support for each PV unit, with reactive power ranges from −25% (absorption) to +25% (injection) of its inverter's apparent power rating, according to the curve shown in Figure 5. In all cases, PV inverter controls are in VAR priority.
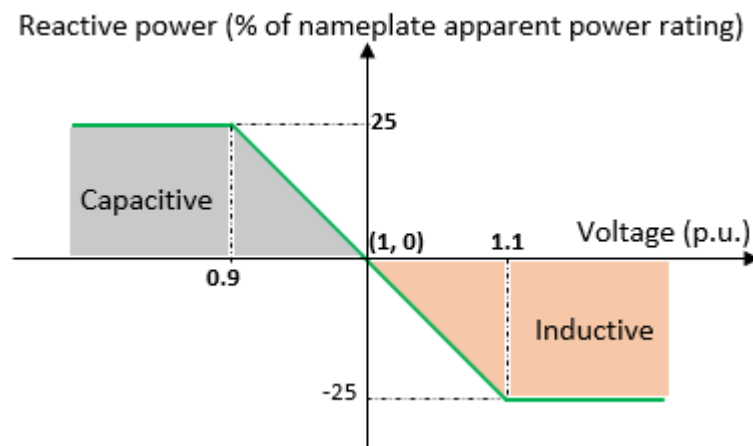
Figure 5. Category A Volt–VAR curve from the IEEE 1547–2018 standard [20].

3.3. ed-LiFo Parameters

The *ed-LiFo PoA* controls are issued every 15 min. The control action issued is enforced for the next 15 min, then updated during the next *ed-LiFo* control iteration.

For the test feeder studied in this paper, according to Equation (10), r must be selected between -0.73 and 9.63. We use two empirically chosen values of r: $r = -0.657$ and $r = -0.58$. The resulting curtailment zone radius values are, 0.00225 and 0.0045 Ω, respectively. The pure *LiFo* case—i.e., the case where all PV units are always considered as curtailment candidates and thus curtailed solely according to their access right—is a particular case in *ed-LiFo*, with $r = \frac{E_{max} - \mu}{\sigma}$, or 9.63 for our test feeder. This corresponds to a curtailment zone radius of 0.175 Ω.

The hypothesis in the assignment of access right is that *PV1* is the first interconnected and *PV3*, the last. Therefore, the *LiFo* curtailment order is {*PV3, PV2, PV1*}, subject to the overload contribution based on the position of each PV unit with regard to curtailment zones dynamically formed during each *ed-LiFo* iteration.

4. Results and Discussion

In this paper, we study voltage and thermal loading impacts of the *ed-LiFo PoA* as well as the curtailment incurred by non-firm PV units. The *ed-LiFo* results are benchmarked against two base cases with the same PV units with unity power and default Category A Volt-VAR control, respectively. Moreover, because of the parametric nature of the *ed-LiFo* concept, we next investigate the sensitivity of each PV unit's annual energy curtailment with respect to the curtailment zone radius. In this paper, the term curtailment, expressed in percent, refers to the annual energy curtailment defined by (11).

$$Curtailment = \frac{AnnualEnergy_{w/oPoA} - AnnualEnergy_{w/PoA}}{AnnualEnergy_{w/oPoA}} \times 100 \qquad (11)$$

where $AnnualEnergy_{w/oPoA}$, is the annual energy produced by a PV unit before the principles of access scheme is applied; and $AnnualEnergy_{w/PoA}$, the annual energy produced by a PV unit after the principles of access scheme is applied.

4.1. Sensitivity of Curtailment Risks and System Efficiency to Curtailment Zone Radius

As shown in the illustrative case of Figure 1 and the subsequent discussion of Equations (7) and (8), the selection of the curtailment zone radius is critical to an efficient active network management. In fact, the value of the curtailment zone radius determines the weight placed on a PV unit's responsibility in a given thermal overload. As *ed-LiFo* operates in a *PoA* framework, finding the best balance between access right and responsibility vis à vis thermal violations is key for a flexible interconnection paradigm based more on which generators are actually contributing to the constraint. Individual non-firm gener-

ation assets can experience very different curtailment risks under different zone radius settings. Figure 6, Figure 7 and Figure 8 show the curtailment distribution for three zone radius values.
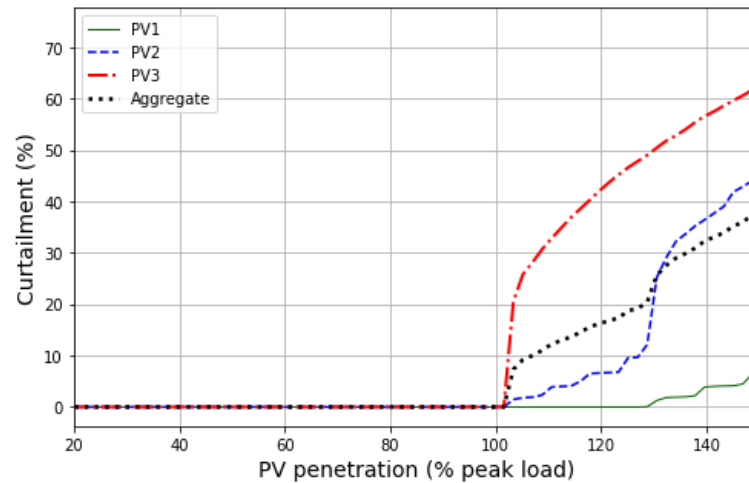

Figure 6. Annual energy curtailment under pure last-in, first-out (*LiFo*) (*ed-LiFo* with 0.175 Ω curtailment zone radius).
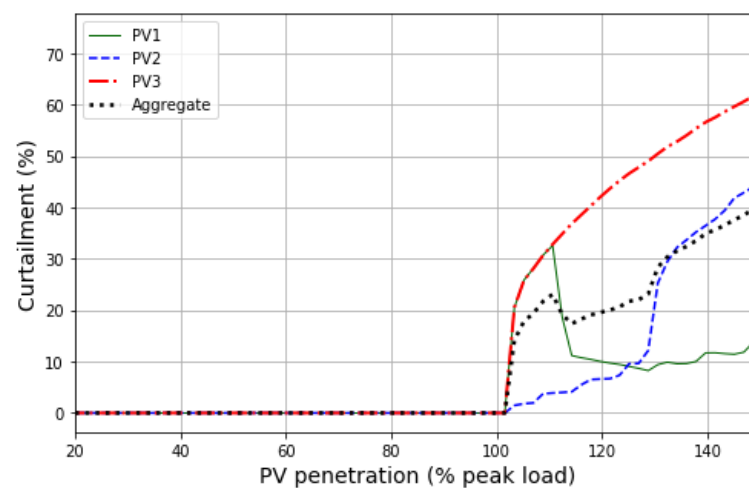

Figure 7. Annual energy curtailment under *ed-LiFo* with curtailment zone radius of 4.5×10^{-3} Ω.

Figure 6 shows the annual energy curtailment of the three utility-scale PV systems under a last-in first-out interconnection agreement as well as the system-wide aggregate curtailment. The index of each PV system reflects its interconnection order. As expected, under this agreement type, where a PV unit's output is curtailed solely based on its interconnection order, the last unit to connect, *PV3*, incurs the highest curtailment risk, whereas *PV1*, the first unit to connect, experiences the least curtailment. Under the *ed-LiFo* agreement, setting the curtailment zone radius to the electrical diameter of the test feeder is equivalent to simply relying on the PV units' interconnection orders or access rights to decide which unit to curtail at a given time. This setting removes the thermal violation contribution factor of individual PV units from the curtailment decision. Note that the aggregate PV energy curtailment is relative to the total PV capacity. As all PV units are of the same size, the aggregate curtailment percentage is the average of the three PV systems. This holds true in Figures 7 and 8.
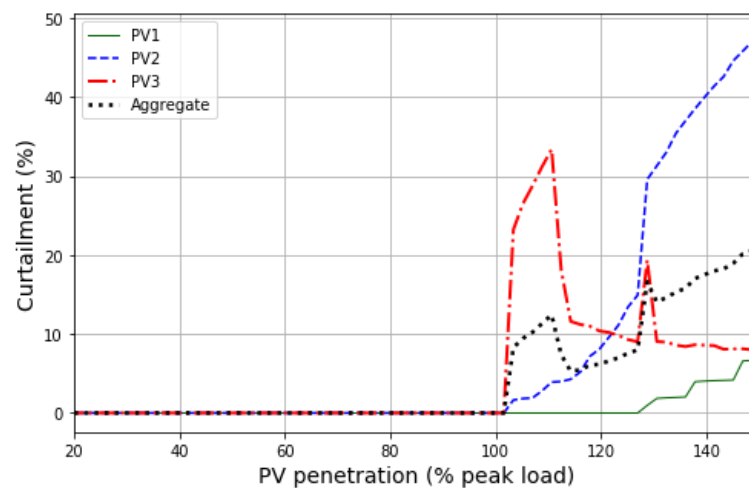
Figure 8. Annual energy curtailment under *ed-LiFo* with curtailment zone radius of $2.25 \times 10^{-3} \Omega$.

To account for the proximity of the PV units to potential thermal overloads, Figure 7 shows the curtailment risk distribution among all three flexible PV units under *ed-LiFo* with a lower curtailment zone radius. The curtailment zone radius is set to $4.5 \times 10^{-3} \Omega$.

The effect of considering the thermal violation contribution factor is explicitly seen at PV penetrations between 102% and 125% of peak feeder load, where *PV1* incurs more curtailment risk than *PV2*. In fact, *PV1* is closer to the overloaded lines more often in this PV penetration range, at the curtailment zone radius of $4.5 \times 10^{-3} \Omega$. The main question is: which curtailment radius would be the most appropriate? Based on the *ed-LiFo* concept, a smaller radius would effectively limit unnecessary curtailment, whereas a higher radius would increase it; however, when no PV unit is found in the vicinity of the thermal overloads, all PV units are curtailment candidates based on their *LiFo* interconnection order. Therefore, extremely small curtailment radius values would lead to the same results as a pure *LiFo* case; however, the radius should be small enough that it truly captures, to some extent, the correlation between thermal violation contributions and curtailment risks incurred. Figure 8 presents an *ed-LiFo* curtailment case where the radius is set to $2.25 \times 10^{-3} \Omega$.

Overall, the PV curtailment is consistently triggered at 102% PV penetration level for all control strategies. The answer to the question "which curtailment radius would be most appropriate, under *ed-LiFo*?", relies not only on the interconnection order but also on the proximity to the overload area (based on the curtailment zone radius). Although the interconnection order is fixed, the proximity to the overload can be tuned by an appropriate setting of the curtailment zone radius, as demonstrated by Figures 6–8. In addition, non-firm generators can incur significant annual energy curtailment risks once a certain penetration level is reached. Figure 9 compares the system-wide aggregate PV curtailments (previously shown in Figures 6–8) of all three presented curtailment radius values.

The aggregate system PV curtailment can be used as an efficiency measure. In fact, the less curtailed energy resource, the better it is for flexible PV unit owners because they would lose less revenue. From a system standpoint, however, if the same thermal violations could be resolved by less resource curtailment, the curtailment scheme deployed would be considered more efficient. Results indicate that more than 45% reduction in total curtailment can be achieved. Even though our case study reveals that the highest curtailment efficiency is achieved with the lowest curtailment zone radius ($2.25 \times 10^{-3} \Omega$), there is no linear correlation between the efficiency and the radius. The highest radius does not necessarily lead to the lowest efficiency (i.e., the highest aggregate curtailment). The choice of the curtailment radius is critical. Future studies will investigate the radius selection problem, with the objective of increasing curtailment efficiency.
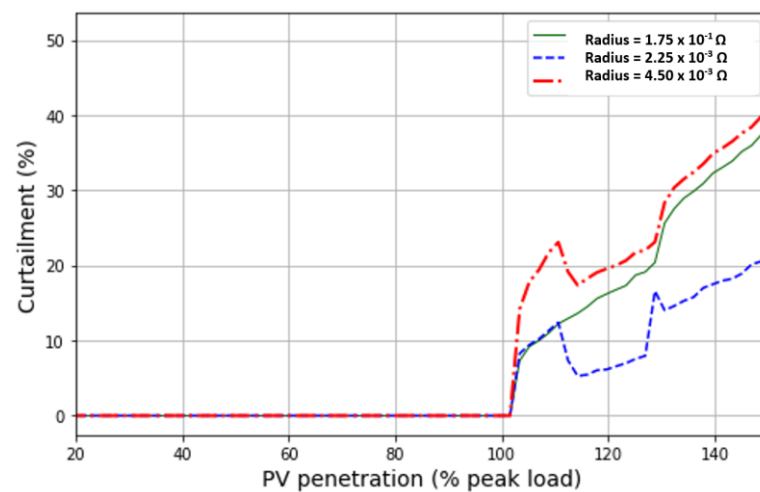
Figure 9. Comparison of aggregate PV energy curtailments for three curtailment radius values.

Given that the *PoA* schemes are aimed toward reducing thermal overloads, it is important to evaluate the impact of flexible generators on other grid operational parameters, such as voltage and power quality. Hence, in addition to studying the effectiveness of *ed-LiFo PoA*, Section 4.2 considers the impact of *ed-LiFo* implementation on voltage across the feeder at different PV penetration levels.

4.2. Effectiveness of ed-LiFo PoA at Resolving Distribution Violations

In this section, we present a comparative study of the voltage and thermal loading across the test feeder at different PV penetration levels under three control strategies: (1) all three PV systems are legacy PVs, i.e., their inverter control is set to unity power factor, labeled "*base-case, PF = 1*"; (2) all three PV systems are Volt-VAR controlled, with the Volt-VAR curve presented by Figure 5, labeled "*base-case, VoltVar*"; and (3) all three PV units are considered flexible and controlled by the *ed-LiFo* scheme introduced in this paper, labeled "*edLiFo, VoltVar*". The reactive power limit of the Volt-VAR curve in the *ed-LiFo* case is 25% of the inverter's rated kVA. The *ed-LiFo* design with radius of 2.25×10^{-3} Ω (see Figure 8) is used. In the first two strategies, the PV units are considered firm generators.

Figure 10 shows the maximum line and transformer thermal loadings by PV penetration for all three control strategies. Regardless of the control strategy, no transformer is overloaded at any time throughout the year at any PV penetration, indicating the effectiveness of the *ed-LiFo* algorithms at resolving thermal overloading issues. If the PV units were to connect as firm generators, however, they would incur the line reconductoring costs for any PV penetration more than 100% whether they use Volt-VAR control, as shown by the maximum line thermal loading curves under *base-case, PF = 1* and *base-case, VoltVar*.

Figure 11 shows the maximum and minimum voltages across the test feeder for different PV penetration levels. The feeder experiences the highest voltages in the legacy PV (*PF = 1*) case. All minimum voltages are within the ANSI A limits. Although the firm generator cases (control strategies (1) and (2)) would require voltage upgrades well before the 20% PV penetration, the *ed-LiFo* case would need to participate in voltage regulation upgrades only after 40% PV penetration, when the maximum voltage reaches the 1.05 *p.u.* upper threshold.
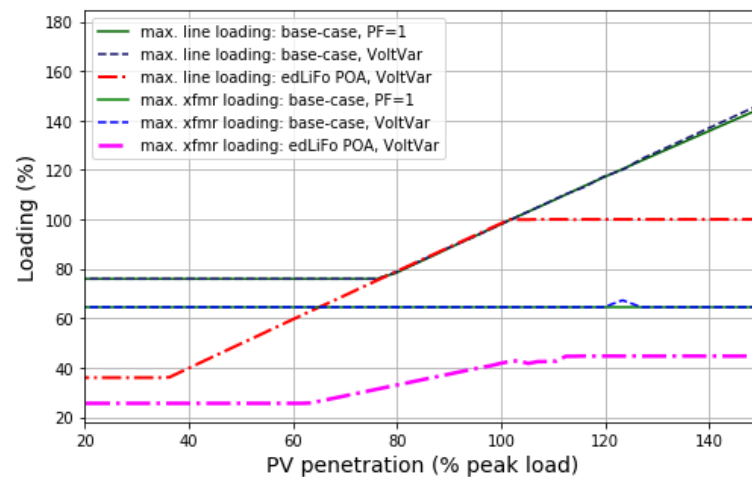
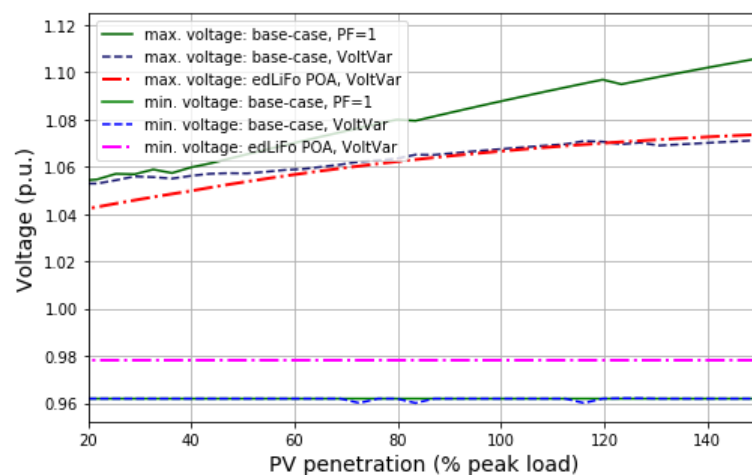**Figure 10.** Line and transformer thermal loading per PV penetration by study case.

Figure 11. Voltage range per PV penetration by study case.

5. Conclusions and Future Work

This paper investigated the curtailment risk of large-scale PV power plants connected to the grid under a flexible interconnection agreement, namely, *ed-LiFo*, a novel *PoA* interconnection option introduced herein. It has been shown that the curtailment risk distribution across flexible generators is fundamentally sensitive to the selected value of the curtailment zone radius. This design parameter of *ed-LiFo* is critical not only to individual flexible generators' curtailment risk but also to system operational resource efficiency because it would impact the amount of flexible generation resource that is unnecessarily curtailed because of the inherent access priority enforced in *LiFo PoA* schemes. The *ed-LiFo* scheme balances the access rights of flexible generators and their estimated responsibility in thermal overloads. The curtailment zone radius is the *ed-LiFo* design parameter that is used to tune the access right and overload contribution balance to increase the fairness of output curtailment among non-firm generators. The test cases considered reveal that non-firm generators under the *ed-LiFo* agreement would not trigger any line reconductoring or transformer replacement upgrade. With a proper choice of curtailment zone radius, utilities can reduce their total flexible PV curtailment by up to more than 45%. The study shows that there is no linear correlation between the system efficiency and the curtailment zone radius. The highest radius does not necessarily lead to the lowest efficiency, i.e., the highest aggregate curtailment. Future studies will research the radius selection problem, with the objective of increasing curtailment efficiency. Future work will also investigate the sensitivity of *ed-LiFo*-induced curtailment to the share of firm generators in overall PV

penetration. Further research will focus on the cost–benefit analysis of the *ed-LiFo PoA* interconnection option for non-firm generators and for utilities.

Abbreviations

A	Electrical adjacency matrix made of conductance parameters
CCPV	Set of curtailment candidate PV units arranged in their LiFo order
CCN	Set of curtailment candidate nodes
D	Electrical "degree" matrix, diagonal matrix
DCN	Set of nodes that are directly connected to any thermal violation
DER	Distributed energy resource
DSO	Distribution system operator
E	Electrical distance matrix
ed-LiFo	Electrical distance-based, last-in, first-out principles of access
g_{ij}	Conductance that connects vertices i and j
L	Conductance matrix, a Laplacian matrix
LiFo	Last-in first-out
$L^\dagger$	Pseudo- or group inverse of the conductance matrix L
μ	Average electrical distance between any two nodes of a feeder
PF	Power factor
PoA	Principles of access
p.u.	Per unit
PV	Solar photovoltaic
QSTS	Quasi-static time-series simulation
ρ	Curtailment zone radius
σ	Standard deviation of the electrical distance between any two nodes of a feeder
S	Apparent power
VoltVar	Volt VAR control function
X/R	X (reactance) by R (resistance) ratio
i, j, k, t, z	Node indices

References

1. Strbac, G.; Jenkins, N.; Hird, M.; Djapic, P.; Nicholson, G. *Integration of Operation of Embedded Generation and Distribution Networks*; University of Manchester Institute of Science and Technology (UMIST): Manchester, UK, 2002.
2. Energy Networks Association. *Active Network Management Good Practice Guide*; Energy Networks Association: London, UK, 2019.
3. Currie, R.; O'Neill, B.; Foote, C.; Gooding, A.; Ferries, R.; Douglas, J. Commercial arrangements to facilitate active network management. In *CIRED 21st International Conference on Electricity Distribution*; CIRED: Frankfurt, Germany, 2011; pp. 6–9.
4. Baringa Partners; UK Power Networks. Flexible Plug and Play Principles of Access Report. December 2012, p. 120. Available online: https://www.ukpowernetworks.co.uk/internet/asset/dac8de6d-1243-4689-b5b5-a8285a2553fe/Principles_of_Access_report_FINAL.pdf (accessed on 2 March 2021).
5. Connect, R.E.V. Lessons from REV Demos in New York's Energy System. 2018. Available online: https://nyrevconnect.com/wp-content/uploads/2018/01/Webinar2_Demo-Principles-v6-01-17-18.pdf (accessed on 17 January 2018).
6. Kane, L.; Ault, G. A review and analysis of renewable energy curtailment schemes and principles of access: Transitioning towards business as usual. *Energy Policy* **2014**, *72*, 67–77. [CrossRef]
7. Anaya, K.L.; Pollitt, M.G. Experience with smarter commercial arrangements for distributed wind generation. *Energy Policy* **2014**, *71*, 52–62. [CrossRef]
8. Dolan, M.J.; Davidson, E.M.; Kockar, I.; Ault, G.W.; McArthur, S.D.J. Distribution power flow management utilizing an online optimal power flow technique. *IEEE Trans. Power Syst.* **2012**, *27*, 790–799. [CrossRef]
9. Currie, R.A.F.; Ault, G.W.; Foote, C.E.T.; McNeill, N.M.; Gooding, A.K. Smarter ways to provide grid connections for renewable generators. In Proceedings of the IEEE PES General Meeting, Minneapolis, MN, USA, 25–29 July 2010; pp. 1–6.
10. Sun, W.; Harrison, G.P. Influence of generator curtailment priority on network hosting capacity. In Proceedings of the CIRED 22nd International Conference on Electricity Distribution, Stockholm, Sweden, 10–13 June 2013. Available online: https://citeseerx.ist.psu.edu/viewdoc/download?doi=10.1.1.1063.6959&rep=rep1&type=pdf (accessed on 2 March 2021).
11. Danzerl, D.; Gill, S.; Kockar, I.; Anaya-Lara, O. Assessment of the last-in-first out principle of access for managing the connection of distributed wind generators. *IET* **2016**, 2–6. Available online: https://strathprints.strath.ac.uk/59906/1/Danzerl_etal_RPG2016_Assessment_of_the_last_in_first_out_principle_of_access.pdf (accessed on 2 March 2021).
12. Jupe, S.C.E.; Taylor, P.C. Distributed generation output control for network power flow management. *IET Renew. Power Gener.* **2009**, *3*, 371–386. [CrossRef]
13. Masters, C.L. Voltage rise: The big issue when connecting embedded generation to long 11 kV overhead lines. *Power Eng. J.* **2002**, *16*, 5–12. [CrossRef]
14. Klein, D.J.; Randić, M. Resistance distance. *J. Math. Chem.* **1993**, *12*, 81–95. [CrossRef]
15. Bu, C.; Sun, L.; Zhou, J.; Wei, Y. A note on block representations of the group inverse of Laplacian matrices. *Electron. J. Linear Algebra* **2012**, *23*, 866–876. [CrossRef]
16. Zhou, J.; Bu, C.; Wei, Y. Group inverse for block matrices and some related sign analysis. *Linear Multilinear Algebra* **2012**, *60*, 669–681. [CrossRef]
17. Ben-Israel, A.; Greville, T.N. *Generalized Inverses: Theory and Applications (Vol. 15)*; Springer Science & Business Media: New York, NY, USA, 2003; Volume 15.
18. Zhang, T.; Bu, C. Detecting community structure in complex networks via resistance distance. *Phys. A Stat. Mech. Its Appl.* **2019**, *526*, 120782. [CrossRef]
19. Horowitz, K.A.; Jain, A.; Ding, F.; Mather, B.; Palmintier, B. A techno-economic comparison of traditional upgrades, volt-var controls, and coordinated distributed energy resource management systems for integration of distributed photovoltaic resources. *Int. J. Electr. Power Energy Syst.* **2020**, *123*, 106222. [CrossRef]
20. Photovoltaics, Distributed Generation, and Energy Storage. IEEE standard for interconnection and interoperability of distributed energy resources with associated electric power systems interfaces. *IEEE Std.* **2018**, 1547–2018. [CrossRef]